**Supplemental Table 1: X-ray data collection and refinement statistics for the ssRNA-LSD1-CoREST structure.**

**Supplemental Data Table 1** Data collection and refinement statistics

| | LSD1-CoREST-ssRNA (PDB: 4XBF) |
|---|---|
| **Data collection** | |
| Space group | $I_{222}$ (23) |
| Cell dimensions | |
| *a*, *b*, *c* (Å) | 123.86, 179.37, 235.05 |
| $\alpha, \beta, \gamma$ (°) | 90.0, 90.0, 90.0 |
| Resolution (Å) | 49.018 – 2.803(2.903 - 2.803) * |
| $R_{merge}$ | 0.031(0.2884) |
| $I/\sigma I$ | 18.9 (2.9) |
| CC1/2 | 0.999(0.873) |
| Completeness (%) | 99.5 (94.0) |
| Redundancy | 12.7(1.9) |
| | |
| **Refinement** | |
| Resolution (Å) | 49.02 – 2.803 |
| No. reflections | 62314 |
| $R_{work}$/ $R_{free}$ | 0.201/0.227 (0.282/0.327) |
| No. non-hydrodgen atoms | 6486 |
| Protein | 6379 |
| Ligand/ion | 84 |
| Ave B-factors | 62.76 |
| Protein/RNA | 62.90 |
| Ligand/ion | 55.26 |
| R.m.s deviations | |
| Bond lengths (Å) | 0.003 |
| Bond angles (º) | 0.74 |
| Rotamer outliers (%) | 0.15 |
| Ramachandran favored (%) | 96 |
| Allowed (%) | 3.5 |
| Outliers (%) | 0 |

Extraction of final model statistics generated in the Phenix
*Highest resolution shell is shown in parenthesis.

**Supplemental Table 2:** Distances between the 5'-UUAG-3' ssRNA fragment and LSD1 residues (PDB 4XBF). Distances (< 3.0 A) are listed and correspond to Figure 5B-D.

| RNA(atom) | LSD1(atom) | distance (Å) |
|---|---|---|
| U1 (O4) | 617 (HN) | 2.0 |
| U1 (O4) | 616 (HA) | 2.5 |
| U1 (H3) | 616 (HA) | 2.9 |
| U1 (H3) | 615 (CO) | 1.8 |
| U1 (H3) | 616 (HA) | 2.6 |
| U1 (H3) | 617 (HN) | 2.9 |
| A3 (N1) | 618 (HA) | 2.8 |
| A3 (H2) | 280 (HG2) | 2.4 |
| A3 (H2) | 280 (HB2) | 2.3 |
| A3 (H2) | 280 (HB3) | 2.2 |
| A3 (H61) | 619 (OD1) | 2.5 |
| G4 (H1) | 619 (OD1) | 2.5 |
| G4 (H1) | 619 (OD2) | 2.9 |
| G4 (H21) | 280 (HN) | 3.0 |
| G4 (H21) | 619 (OD2) | 2.1 |
| G4 (H21) | 279 (HA2) | 2.8 |

**Supplemental Figure 1**: **Purity of full-length LSD1, CoREST, and LSD1-CoREST constructs prepared for this study. A)** Schematic of LSD1 (top) and CoREST (bottom). LSD1 contains a SWIRM domain, an intertwined oxidase domain (cyan, blue) that performs the lysine specific demethylase catalytic reaction, and a tower domain (green) that forms a key coiled-coil interaction with CoREST. CoREST contains an ELM2 domain and two SANT domains. Whereas demethylation kinetic studies were performed with full-length LSD1, all EMSA, cross-linking, and structural studies (**Figures 3 - 5**) were performed with truncated LSD1-CoREST (pink boxes). **B)** SDS-PAGE gel of the purified full-length LSD1. **C)** SDS-PAGE gel of the truncated CoREST (286-482). **D)** SDS-PAGE gel of the purified LSD1-CoREST complex using size exclusion chromatography (Superdex 200 10/300 GL). **E)** The analysis of analytical ultracentrifugation (AUC) data of the LSD1-CoREST complex. The plot shows the continuous distribution (C(s)) versus the sedimentation distribution coefficient (S), revealing the presence of a stable, intact, stoichiometric 1:1 complex. The residual distribution histogram from the AU analysis is shown in the upper right corner.

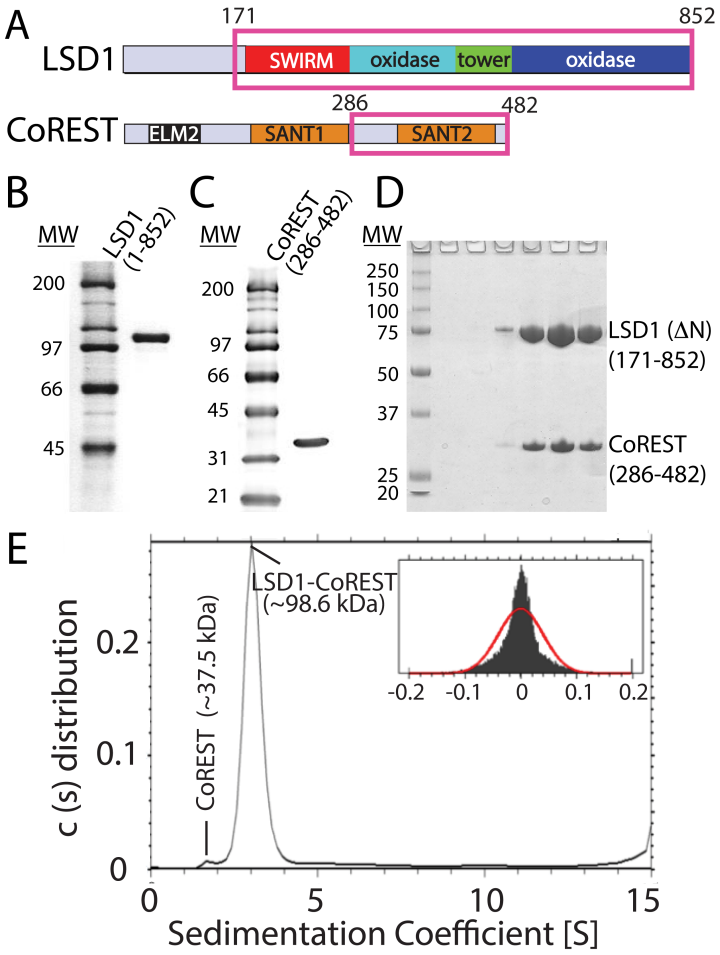

**Supplemental Figure 2: Monovalent ions dramatically influence the global structure of the 5'-GG[UUAGGG]$_4$UUA-3' RNA. A**) Circular dichroism spectroscopy demonstrates that parallel-stranded GQ structures form in the presence of potassium (blue) and sodium (green), consistent with previous studies (Balaratnam and Basu 2015). In contrast, lithium (black) strongly destabilizes GQ formation. **B)** The analysis of deconvoluted analytical ultracentrifugation (AUC) data of the 5'-GG[UUAGGG]$_4$UUA-3' RNA in the presence of potassium (top panel), sodium (middle panel), and lithium (bottom panel). Each plot shows the continuous distribution (C(s)) versus the sedimentation distribution coefficient (S) and the observed peaks indicate a single quadruplex (1), a stacked quadruplex (2), or a broad heterogeneous profile in the case of $Li^+$. The residual distribution histogram for each plot is shown in the upper left or right corners.

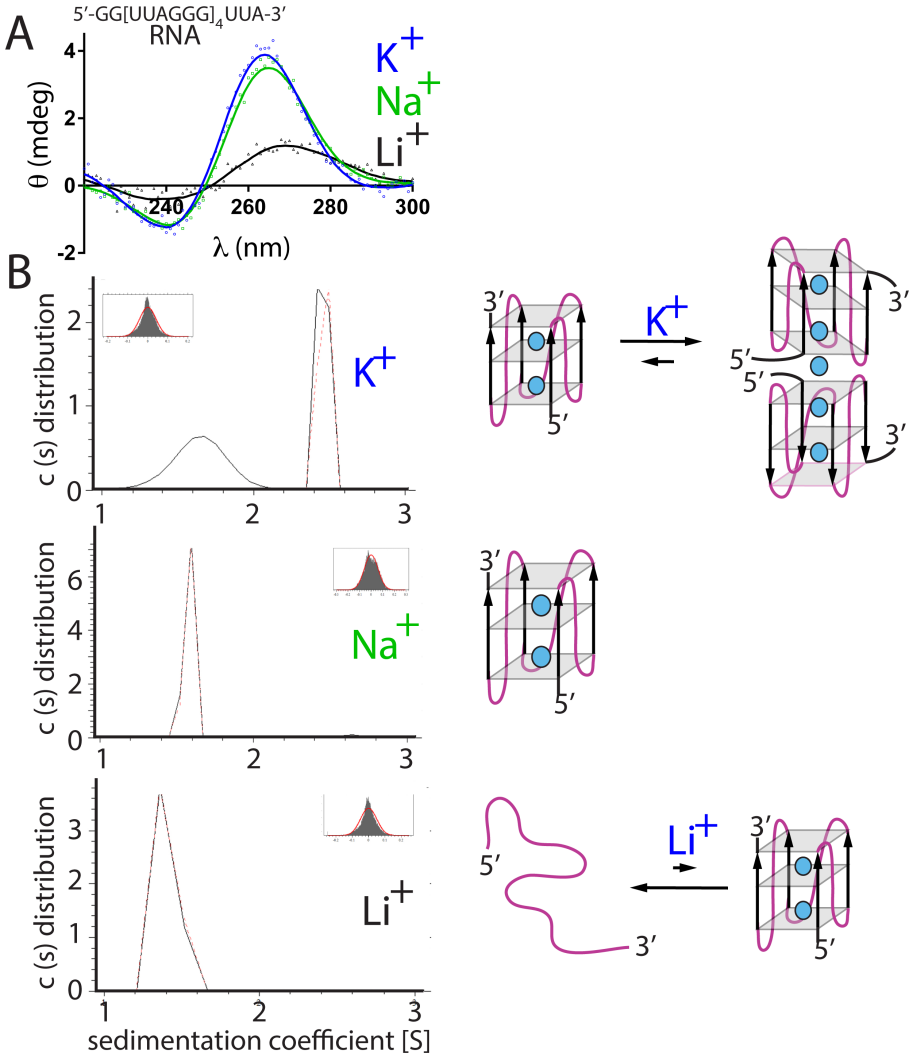

**Supplemental Figure 3: Nucleic acid binding specificity of LSD1 A)** Affinity of LSD1-CoREST binding to a 25 nt GQ forming [$(TTAGGG)_4T$] DNA (box). The plot shows the concentration of the LSD1-CoREST complex versus fraction of RNA bound. Binding studies were assayed in triplicate and representative data are shown in B. **B)** Nucleic acid binding activity of LSD1-CoREST (amino acid residues 171-852 and 286-482, respectively). Complexes and free oligonucleotides were resolved on a 0.75% native agarose gel. The concentration of the LSD1-CoREST complex is noted for each lane (nM) and the dissociation constant ($K_d$) and Hill coefficient (*h*) are shown. **C)** Independent LSD1 and CoREST binding to [$(UUAGGG)_4U$] RNA. Analysis of gel-mobility shift assay binding curves of a 25 nt. GQ forming RNA ($K^+$) with full-length LSD1 only (green), or with CoREST (286-482) (pink). The plot shows the protein concentration of LSD1 or CoREST versus fraction bound. Binding dissociation constant ($K_d$) and Hill coefficient (*h*) are shown. All EMSAs in Supplemental Figure 3 were performed with a 6x His tag located at the C-terminus of CoREST. Fraction bound for LSD1 alone saturates at approximately 60-65%, which may be due to GQ RNA heterogeneity or instability of the LSD1-GQ RNA complex at high micromolar concentrations.

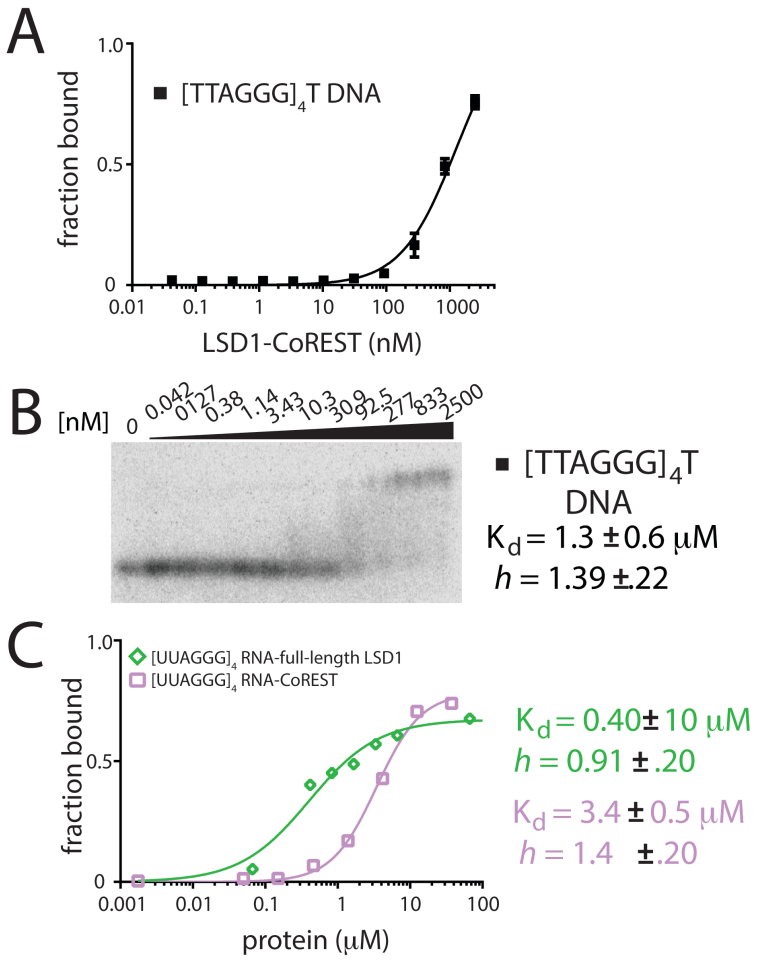

**Supplemental Figure 4: Inhibition of LSD1-catalyzed demethylation. A**) Half maximal inhibitory concentration ($IC_{50}$) profiles for a 25 nt. $[UUAGGG]_4U$ RNA (red), TERRA-like $[TTAGGG]_4T$ DNA (grey), and ssRNA (blue) oligonucleotides are shown, corresponding to apparent $IC_{50}$ values of 0.98, 2.65, and 9.10 μM, respectively. A weak apparent IC50 was also observed for a 5 nt. 5'-UUAGG-3' RNA (black) ($IC_{50}$ ~ 25 μM). This inhibition trend correlates with the affinity-binding trend (Figure 3, Supplemental Figure 3). Analysis of the log (inhibitor) dose-response curves identified the $IC_{50}$ values for each inhibitor. **B)** Non-competitive inhibition of LSD1 by TERRA RNA. Increasing amounts of a 25 nt. TERRA RNA (0 μM (black), 1.5 μM (pink), 2.5 μM (red)) show a decrease in maximal velocity ($V_{max}$) but no change in the $K_M$. By measuring $k_{observed}$ at different substrate concentrations for each amount of RNA, apparent $V_{max}$ and $K_M$ values can be obtained. Experiments were performed in duplicate and were performed in the absence of CoREST.

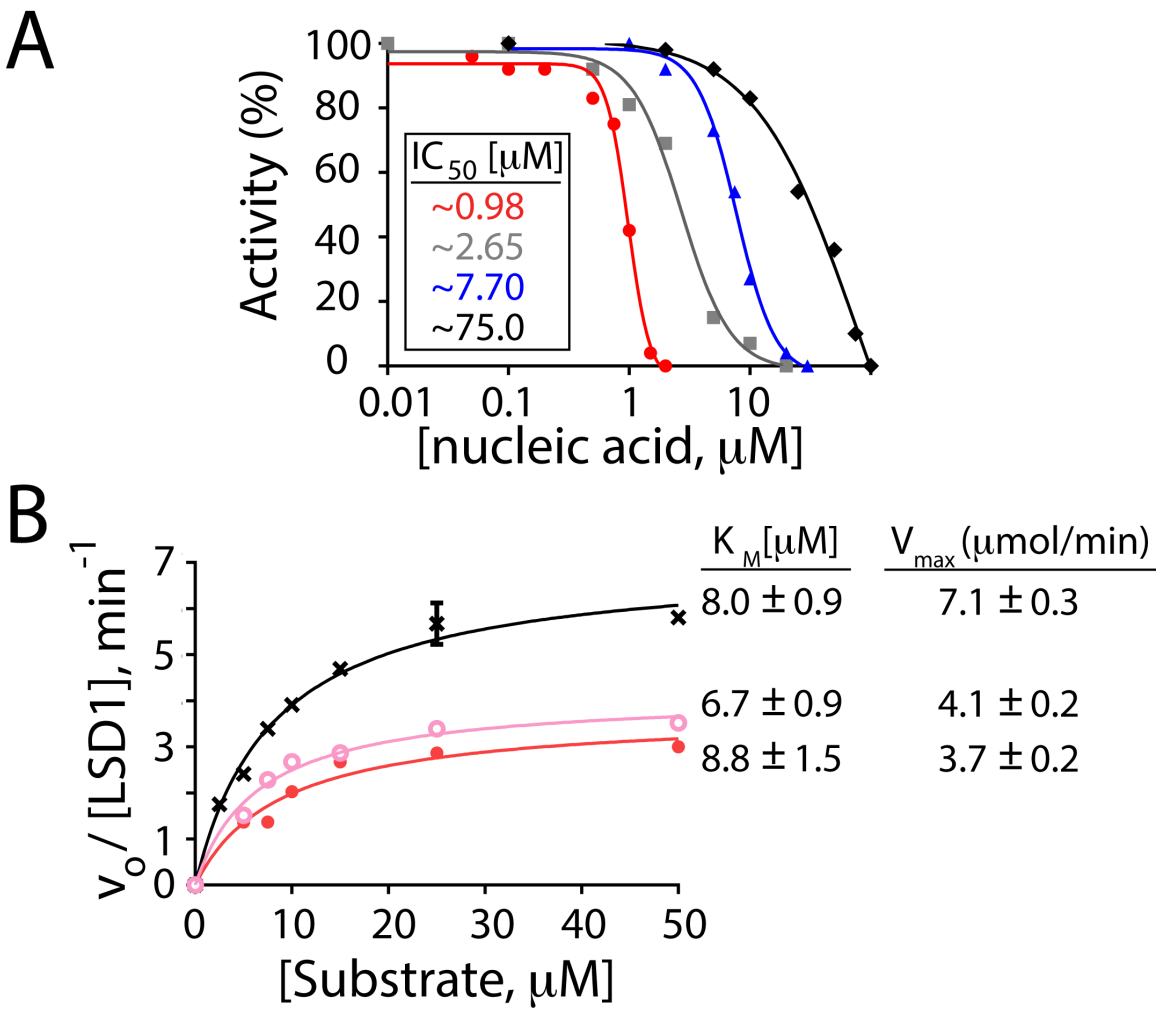

**Supplemental Figure 5: Identification of candidate GQ binding regions on LSD1 via cross-linking mass spectrometry.** LSD1-CoREST was irradiated with 254 nM UV light either alone (control) and in the presence of a 5' biotinylated GQ RNA. Streptavidin beads were used to isolate LSD1 covalently bound to the RNA. The control protein and RNA-protein complex were SDS-PAGE purified, trypsin digested, and analyzed using high resolution LC-MS/MS. Two separate crosslinking LC-MS/MS experiments on two freshly purified LSD1-CoREST samples were performed to elucidate the primary LSD1 regions that crosslink with RNA. **Raw Data (A-B). A)** The LSD1 peptide fragment (227-251) from the GQ RNA cross-linked sample was ~10,000 fold weaker than in the control, indicating that the mass of this peptide has been altered due to RNA adduction. **B)** Representative analysis of an LSD1 peptide fragment (486-492) that does not crosslink to RNA. The change in intensity between the control LSD1 sample and the LSD1-RNA crosslinked sample is modest (20-fold weaker) and is equivalent to the difference in total mass injected. For A and B, the m/z ratio and calculated isotope dot product values confirm the identity of the peak based on the expected isotopic distribution (M, M+1, M+2, M+3). **Peptide analysis and coverage for separate crosslinking-MS experiments (C-D) C)** Plot of the ratio of control to cross-linked sample by LSD1 amino acid residue. Three peptide regions are depleted in the RNA-LSD1 cross-linked sample (LSD1 regions (227-251), (527-550), and (695-720). The significant change in the m/z ratio and elution profiles of the RNA-bound peptide result in the depletion of peptide signal. A plot of the total abundance ($Log_{10}$) of the peptides in each sample reveals relatively consistent coverage of the control LSD1 (blue bar) and the RNA cross-linked LSD1 (black). This LSD1-CoREST sample contains a 6x His-tag located the C-terminus of CoREST and was crosslinked with a single GQ forming 5' biotinylated RNA (GUUU$(UUAGGG)_4$UUA). **D)** A separate RNA-LSD1 crosslinking MS experiment reveals two peptide regions that are depleted in the RNA-LSD1 cross-linked sample. These two regions were previously observed in **C** and represent LSD1 regions (227-251) and (527-550). In contrast to the sample analyzed in **C**, this LSD1-CoREST sample does not contain a 6x His-tag located the C-terminus of CoREST and used a stacked GQ forming 5' biotinylated RNA (5′ biotinylated GGG$(UUAGGG)_8$UUA). Analysis of **C** and **D** were performed in an identical manner.

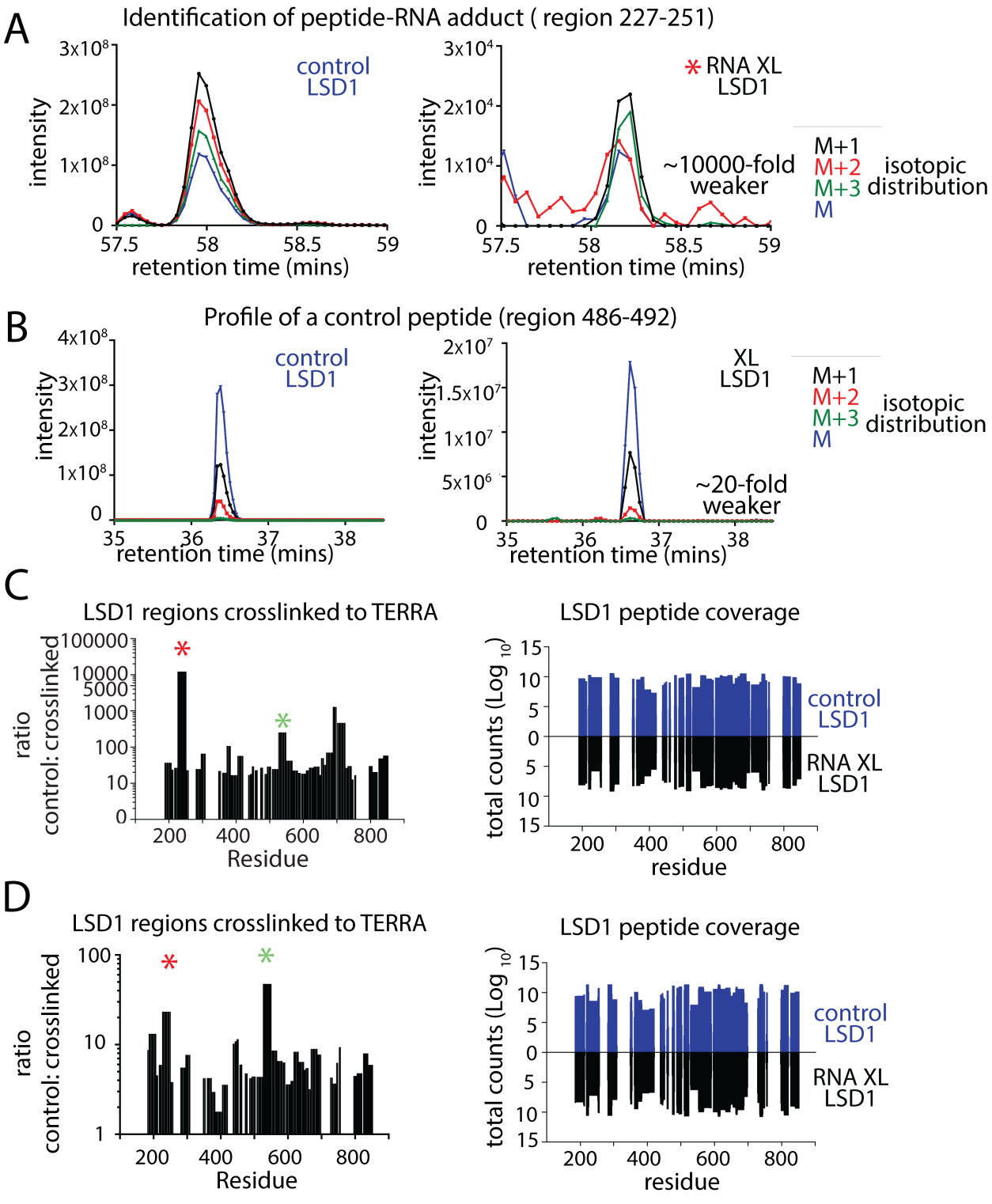
A
Identification of peptide-RNA adduct ( region 227-251)
intensity
control
LSD1
retention time (mins)
RNA XL
LSD1
~10000-fold
weaker
M+1
M+2
M+3
M
isotopic
distribution
B
Profile of a control peptide (region 486-492)
control
LSD1
XL
LSD1
~20-fold
weaker
C
LSD1 regions crosslinked to TERRA
ratio
control: crosslinked
Residue
LSD1 peptide coverage
total counts (Log 10)
residue
D
LSD1 regions crosslinked to TERRA
LSD1 peptide coverage

**Supplemental Figure 6: UV Light specifically cross-links LSD1-CoREST to a stacked GQ RNA.** A 5' $^{32}$P-labeled 5'-GG[UUAGGG]$_8$UUA-3' RNA and a size matched, non-GQ forming RNA were incubated with or without ΔN LSD1-CoREST. All RNA concentrations were equivalent. Upon cross-linking at 254 nm, the stacked GQ RNA co-migrates with both ΔN LSD1 and CoREST (Lane 4). The higher molecular weight species indicate a degree of oligomerization. Very faint bands can be observed for the equivalent control RNA (Lane 8), likely the result of low levels of non-specific RNA binding.

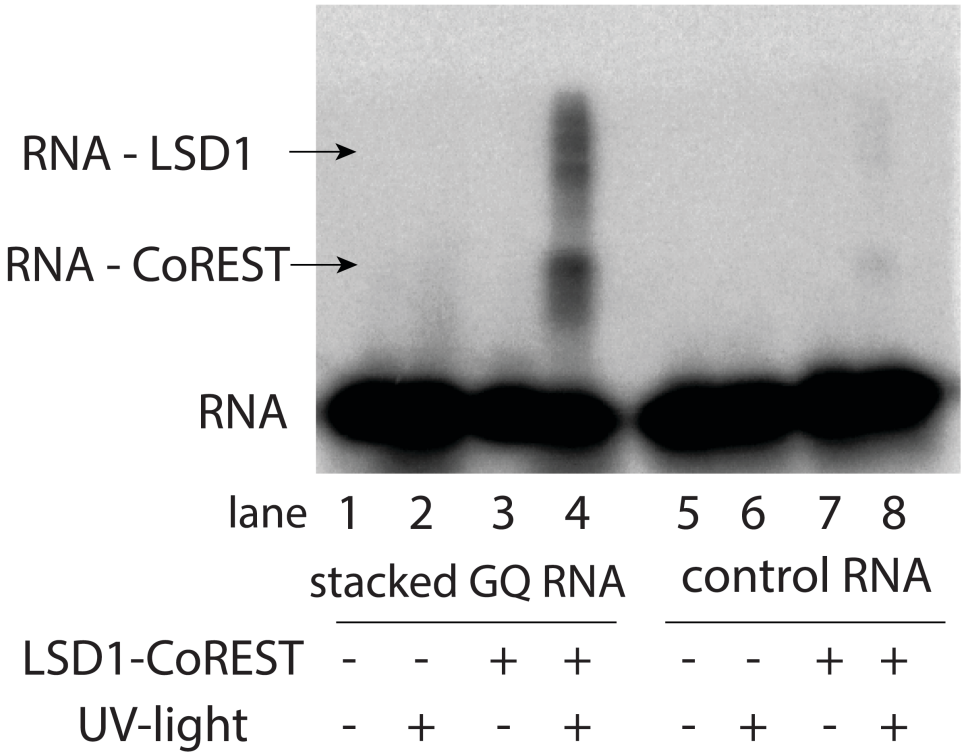

**Supplemental Figure 7:** Difference Fourier map ($|F_o|$-$|F_c|$) unambiguously identifies the location of an ssRNA binding site within the LSD1-CoREST crystals. A mirror view of the monoamine oxidase and SWIRM domains reveal regions of density that correspond to the ssRNA molecule. Other electron density regions were identified as ordered sulfate and water ions. The difference electron density is shown as a dark grey mesh and is contoured at 5.0 r.m.s.d.